Flexure compensation simulation tool for TMT-WFOS Spectrograph

Arun Surya, Matthew Radovan, Sivarani Thirupathi, S. Sriram, Devika Divakar, et al.

Arun Surya, Matthew Radovan, Sivarani Thirupathi, S. Sriram, Devika Divakar, Jason Fucik, "Flexure compensation simulation tool for TMT-WFOS Spectrograph," Proc. SPIE 10705, Modeling, Systems Engineering, and Project Management for Astronomy VIII, 107051G (10 July 2018); doi: 10.1117/12.2312155

SPIE.

Event: SPIE Astronomical Telescopes + Instrumentation, 2018, Austin, Texas, United States

Flexure Compensation Simulation Tool for TMT-WFOS Spectrograph

Arun Surya[a], Matthew Radovan[b], Sivarani Thirupathi[a], S. Sriram[a], Devika Divakar[a], and Jason Fucik[c]

[a]Indian Institute of Astrophysics, Bangalore , India
[b]UCO/Lick Observatory, Univ. of California, Santa Cruz, United States
[c]Department of Astronomy, California Institute of Technology, United States

ABSTRACT

The Wide Field Optical Spectrograph (WFOS) is one of the first-light instruments of Thirty Meter Telescope. It is a medium resolution, multi object, wide field optical spectrograph. Since 2005 the conceptual design of the instrument has focused on a slit-mask based, grating exchange design that will be mounted at the Nasmyth focus of TMT. Based on the experience with ESI, MOSFIRE and DEIMOS for Keck we know flexure related image motion will be a major problem with such a spectrograph and a compensation system is required to mitigate these effects.

We have developed a Flexure Compensation and Simulation (FCS) tool for TMT-WFOS that provides an interface to accurately simulate the effects of instrument flexure at the WFOS detector plane (e.g image shifts) using perturbation of key optical elements and also derive corrective motions to compensate the image shifts caused by instrument flexure. We are currently using the tool to do mote-carlo simulations to validate the optical design of a slit-mask concept we call Xchange-WFOS, and to optimize the flexure compensation strategy. We intend to use the tool later in the design process to predict the actual flexure by replacing the randomized inputs with the signed displacement and rotations of each element predicted by global Finite Element Analysis (FEA) model on the instrument.

Keywords: Spectroscopy, Instrumentation

1. INTRODUCTION

Flexure in spectrographs, at the very least, causes image motion of the spectra at the detector, reduced spectral resolution, and degraded line profiles and estimates of radial velocities. These effects are discussed in detail by Walker and D'Arrigo.[1] Such flexure related degradation can be avoided by using active (Kibrick 2004[2]) or passive (Sheinis A. 1999[3]) flexure compensation systems that use controlled movements of components in the spectrograph to compensate the image motion. Active flexure compensation system mostly use optical real time feed-back to measure error to control active compensating elements in the spectrometer. Passive compensation involves modeling and calibrating the flexure of the instrument to determine a predefined solution for the compensation of controlled elements which is a function of the instrument position relative to gravity.

The Wide Field Optical Spectrograph (WFOS)[4,5] is one of the first-light instruments of Thirty Meter Telescope (TMT). WFOS is a seeing-limited, wide-field imaging multi-object spectrometer. WFOS is expected to capture medium-resolution (R = 5,000) spectra in two or more color channels simultaneously, spanning 310 - 1100nm passband. We discuss the development of a Flexure Compensation and Simulation (FCS) tool that provides an interface to accurately simulate the effects of instrument flexure at the WFOS detector plane, using perturbation of key optical elements and also derive corrective motions to compensate the shifts caused by instrument flexure. We are currently using the tool to simulate the expected image motion in the focal plane and to explore which optical elements are needed to be actively compensated to correct the flexure.

Further author information: (Send correspondence to A.S.)
A.S.: E-mail: arunsuryaoffice@gmail.com

Modeling, Systems Engineering, and Project Management for Astronomy VIII
edited by George Z. Angeli, Philippe Dierickx, Proc. of SPIE Vol. 10705
107051G · © 2018 SPIE · CCC code: 0277-786X/18/$18

We also discuss the sensitivities of optical elements of WFOS with flexure and present the efforts towards modeling a realistic flexure effect and compensation scheme. WFOS will be mounted on the TMT Nasymth platform. Though the entire instrument is mounted on a the Nasmyth platform which has a stiffness requirement, the instrument needs to rotate with respect to the optical axis of the telescope during observations in order to correct for the field rotation. This will introduce rotator dependent flexure during a science observation and will cause a shift of the image position on the detector. This image shift can be corrected in a closed-loop or open-loop manner similar to many instruments on the 8-10m telescopes. The current version of the tool uses a grid of models generated using ZEMAX for a known amount of flexure of key optical components (called the sensitivity maps). These pre-calculated grids of sensitivity maps were generated over the entire WFOS field and wavelength range and are used to generate various combinations of perturbations and a realistic image motion due to flexure. The tool is then used to analyze possible compensation schemes using few active elements. We describe the tool, its performance, assumptions and next steps of improvements in this article. We also discuss how the tool could be used for other large telescope instruments where modeling of flexure induced optical distortions is critical.

Because monolithic slit-based wide field opical spectrometers for ELTs like Xchange-WFOS require optical systems which have unprecedented size,there is a parallel effort to develop a fiber based concept that employs a zonal positioning system and replicated stationary spectrometers to combat flexure. This is discussed elsewhere at these proceedings.[6]

2. MOTIVATION FOR FCS TOOL

The history of WFOS stretches from 2005 to the present, during which time a number of concepts were studied. The most significant being the Multi-Object Broadband Imaging Echellette (MOBIE) which spanned 2008 to 2015.

MOBIE was designed to directly image or create low (R = 1000) to medium-resolution (R = 8,000) spectra in two color channels simultaneously, spanning 310-550nm and 500-1100nm passbands respectively. MOBIE was designed with a rectangular field of approximately 3.0 arcmin x 8.3 arcmin resulting in a field area of 24.9 square arcminutes, and a total slit length of 500 arcsec. The MOBIE optical design was unique because operated in a quasi-littrow configuration relying only on a huge grating β angle (18-23 degrees) to create the required beam clearance between the incoming 300mm diameter collimated beam and the outgoing beam to the massive 440mm diameter refractive cameras. This had the unintended consequence of creating significant variable anamorphic magnification along the slit which resulted in field dependent motion (distortion) of spectra when elements move due to gravity. This effect was something not which had not been previously encountered during the design, modeling and construction of other WM Keck spectrometers and was a surprise to the team. Zemax simulations for points covering the entire MOBIE field of view created complicated distortion patterns which were not correctable by any simple and obvious active flexure compensation solution. We therefore set out to develop the flexure compensation tool to simulate the flexure and to determine if a reasonable active flexure compensation system could be built to correct the flexure in WFOS.

During what was referred to as the Opto-Mechanical Design and Requirements(OMDR) phase (2015-2016), a new team focused on the end-to-end optical design and key mechanical trade-offs to simplify the design. We also advanced the FCS tool while studying ways to reduce the distortion sensitivity of the optical design and ultimately settled on an optical design which reduces the β angle from the 21 degree average in the MOBIE design to 9 degrees for the OMDR design. The new OMDR WFOS design used all the same dispersing components (echelle gratings and prisms for cross dispersion) as the MOBIE design but created the required collimated beam clearance by moving off the Littrow configuration. This helped reduce the distortion sensitivity but created additional geometric vignetting at the mouth of the refractive cameras in one axis. The new OMDR design required the same amount of pupil relief (620mm) as the MOBIE design to clear the incoming beam to the grating but was now significantly more vignetted for a 440mm camera aperture. Larger cameras (550mm) were considered to eliminate the significant geometric vignetting and were found to be feasible for both the red and blue channels. Although the needed material, especially CaF2, can likely be used to build 500mm camera, the cost and risk associated with attempting to build astronomical cameras of this unprecedented size was deemed too risky so the team began to consider a third and a fourth option

Following the OMDR phase of WFOS the project entered a 10 month long trade study (2017-2018) phase to evaluate a Volume Phase holographic (VPH) grating based concept for a long slit instrument which used multiple reconfigurable slicer IFUs to take multiplexed medium resolution spectra with a stationary refractive camera. A second, Fiber IFU based concept with replicated fixed resolution spectrometer was also studied as an option to the long slit spectrometer. During the last two months of the trade-study phase a third concept we called Xchange-WFOS became the front runner for a slit based approach replacing Slicer WFOS. Like the original MOBIE design, this concept has an off-axis slit mask and collimator, two color channels, large refractive cameras, and a linear ADC. Like MOBIE and OMDR WFOS, Xchange-WFOS needs to rotate to track telescope field rotation and will need an active flexure compensation system. Because the FCS simulation tool is flexible as described below, the team was able to use it to analyze MOBIE, OMDR WFOS and Xchange-WFOS. The simulation presented below to demonstrate the FCS tool are all for the Xchange design. The Optical layout (Figure 1) and mechanical layout (Figure 2) are shown for reference below however this tool, by design, can be applied to almost any spectrometer design.

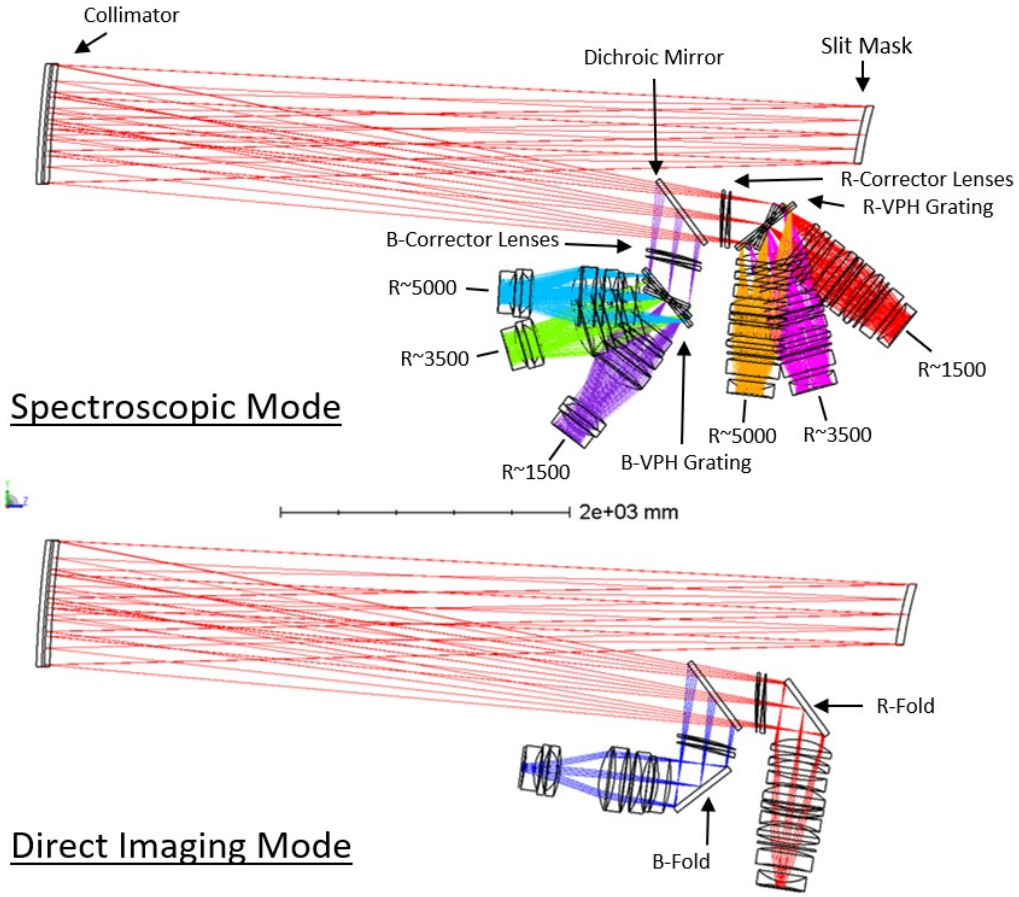

Figure 1. The optical layout for the Xchange-WFOS spectrograph concept.

3. FLEXURE COMPENSATION IN W.M. KECK OBSERVATORY SPECTROGRAPHS

Instrument flexure is a concern for all spectrometers which must work in a changing gravity vector. In the last 20 years several spectrometers have been built on 8-10m class telescope with active or passive flexure compensation systems in an attempt to mitigate gravity induced negative effects of spectra stability and image quality. At the W.M. Keck Observatory there are two (ESI and MOSFIRE) spectrometers operating at the cassegrain focus and

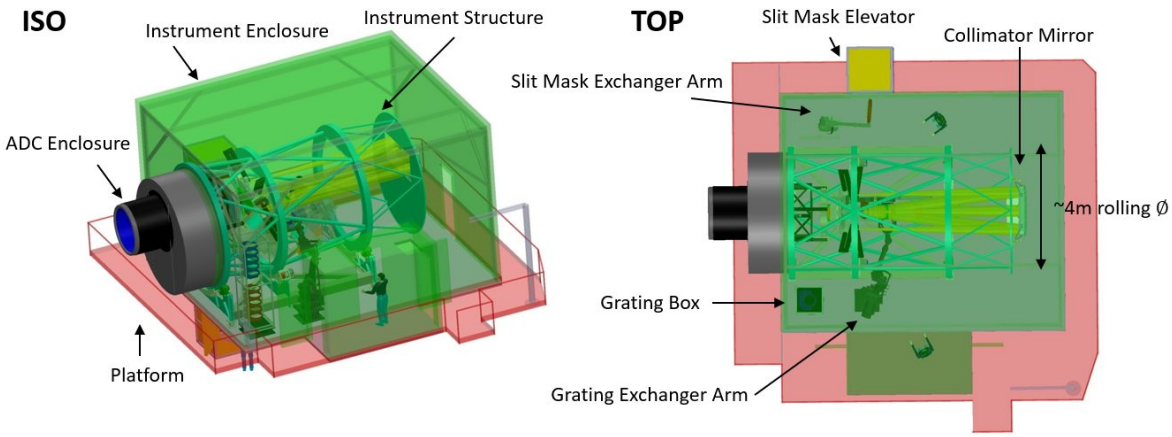

Figure 2. The mechanical layout for the Xchange-WFOS concept.

one instrument (DEIMOS) at Nasmyth focus all of which have active flexure compensation systems. Two of these Keck instruments were built concurrently at UC Santa Cruz. DEIMOS and ESI both have flexure compensation systems to counter act the effects of gravity. ESI is an open-loop system and DEIMOS is closed loop. DEIMOS was designed using Autocad in 2-D. ESI used the same CAD tool but choose to exploit the newly developed 3-D capabilities of the design software. ESI on sky performance is 3.5 times (Table 1) better than DEIMOS despite the fact that it is designed to work at cassegrain focus which a more demanding requirement. Despite the unexpectedly large flexure in DEIMOS, the closed loop system works reasonably well (0.5 pix residual) to correct flexure. However, this is only accomplished by following a very specific protocol for grating exchanges and instrument setup which adds significant over-head to an observation. These procedures were necessary because the native instrument flexure exceeded the capture range of the system which was designed to be twice the instrument flexure budget. What is more significant, when comparing ESI to DEIMOS, is how the predicted and actual flexure compares. ESI's actual flexure performance is only 12 percent greater than the prediction compared to DEIMOS which is 4.2 times (420%) greater than the prediction. Much of the difference between the predicted vs actual performance of the two instruments is intrinsic to the design and modeling philosophy. If the TMT Science Advisory Committee choses to build traditional slit spectrometer to satisfy the WFOS requirements it likely will be an open loop system like the one built for ESI which has proven to be the most reliable and best performing flexure compensation system in a Keck instrument.

MOSFIRE was built by Caltech after ESI and DEIMOS were fully commissioned. It benefited from the development of modern 3-D CAD systems with integrated FEA tools but faced an additional significant challenge, which was not an issue for the ESI or DEIMOS, that MOSFIRE is cryogenic. Because cryogenic instruments have long cool down cycles it is time consuming to investigate and fix issues during factory testing. It is also more difficult to add measured inputs into the system to check the actual response vs the predicted response. During the construction and testing of ESI the spring scale proved to be an invaluable tool. We used it to push and pull on nodes while taking spectra. The resultant image motion was compared to the expected results for FEA simulation of the same disturbance. This allowed us to find soft spots in the structure and helped validate the FEA predictions. This method is nearly impossible to use on a sealed cryogenic instrument. Although the uncorrected flexure in MOSFIRE in one axis was 3.6 times greater than the prediction, the open loop flexure compensation system was able to correct the system to 0.1 pixels everywhere on sky which met the specification. Although MOSFIRE was delivered without a complete understanding of why the modeled and actual performance didnt agree, the MOSFIRE team accomplished the key goal for any open loop system which is to build it without hysteresis.

In summary, all three Keck instrument discussed experience image motion in the spectral format on the CCD during normal operation; however, this motion is distortion free. Controlling flexure has been a major challenge for all these instruments. ESI and MOSFIRE choose a similar approach to predict, optimize and correct for

Instrument	Flexure Prediction pixels(arcsec)		Measured Flexure pixels(arcsec)		CCD scale arcsec/pixel	Residuals after FCS
	Major Axis	Minor Axis	Major Axis	Minor Axis		
ESI	4.8(0.75)	3.8(0.59)	5.4(0.84)	3.4(0.53)	0.156	0.1 pix (0.016 arc sec)
MOSFIRE	3(0.54)	3(0.54)	10.9(1.96)	2.2(0.40)	0.18	0.1 pix (0.018 arc sec)
DEIMOS	6(0.71)	6(0.71)	17(2.02)	6(0.71)	0.119	0.5 pix (0.060 arc sec)

Table 1. DEIMOS, ESI, and MOSFIRE predicted and measured flexure comparison.

flexure. Of the three Keck instruments with active flexure compensation, ESI has the lowest overall flexure and the best agreement with the predicted vs actual performance. It is also the instrument the WFOS team is most familiar with and is therefore logical starting point for thinking about how to design and build WFOS.

3.1 Open vs Closed Loop FCS

Open and closed loop flexure compensation systems have been used on Keck spectrographs with varying degrees of success as previously discussed. All three instruments have active elements which move to correct gravity induced image motion at the CCD. ESI and MOSFIRE are controlled open-loop and hence their performance is critically dependent on residual hysteresis. While an open loop system is conceptually simpler, it requires precision engineering, accurate modeling, and meticulous execution to avoid hysteresis that will limit the performance. ESI compensates for image motion by actively tipping and tilting the collimator whereas MOSFIRE tips and tilts a piezo transducer actuated fold mirror. Closed loop flexure compensation systems are preferred by some people because they can operate in real time and provide feedback to correct for image motion which is not simple flexure effect like thermally induced image motion and are immune to hysteresis. Closed loop systems are usually more complicated and costly due to the extra hardware and software required to monitor the flexure in real time. Closed loop systems require a feedback mechanism which is commonly implemented as a reference signal which follows the same optical path as the science spectra to account for all optical elements. The DEIMOS control loop is closed by monitoring the motion of 4 artificial stars in the focal plane which are created with optical fibers and copper-argon lamps. The spectra for these fibers lands on small FC CCDs which lie on both edges of the focal plane along the spatial axis of the science CCD mosaic. The DEIMOS system requires extra hardware for the closed loop control (fibers, flexure compensation CCD, extra detector electronics) and the system introduces light into the spectrometer from the beacon which can contaminate the star sources if not properly controlled. To simulate a DEIMOS style FCS system the FCS tool includes an option to only use the spectra from the edges of the field.

3.2 Scaling Flexure Values for WFOS

Structural scaling laws can be used to give early insight into the expected flexure performance of WFOS. For a beam with characteristic dimensions L (beam length), b (beam width), h (beam depth), P (end load from gravity acting on a mass at the end of the beam) the deflection (δ) and rotation (θ) of the supported mass are:

$$\delta = \frac{PL^3}{3EI}, \theta = \frac{PL^2}{2EI}, \tag{1}$$

where E is the beam's modulus of elasticity and I is the area moment of inertia of the beam. If a scale factor of S is applied to all dimension the load P will increase by S^3. It can be shown that θ will scale as S and δ will scale as S^2.

While it is sometimes necessary to build structures which have bending, this is not the preferred structure for the major WFOS systems. Truss structures which carry loads only in tension and compression offer a huge advantage over more traditional plate structures which have bending. For the truss structure the axial deflections (δ) of elements are:

$$\delta = \frac{PL}{AE}. \tag{2}$$

	ESI	WFOS	Ratio
Instrument Rolling Diameter	2m	3.5m	1.75
Collimated Beam Size	153mm	300mm	2
Largest Camera Element (dia)	300mm	440mm	1.5
Collimator Distance Diagonal Dist	635mm	1.8m	2.8
Grating Dimensions	200 x 200 mm	300x500 mm	1.5 x 2.5
Mass	2T	16T/32T for S=2/2.5	N/A

Table 2. WFOS and ESI Dimensional Comparison

Although these structures obey the same scaling laws as the simple cantilever beam, they use material much more efficiently and when properly designed have much higher specific stiffness than structures in bending. ESI took this a step farther and built determinate structures (hexapods) to connect all optical elements. These structures do not transfer bending moments between objects being acted on by gravity.

The last consideration for extrapolation of 10m instrument flexure performance is value estimated for S. Examination of ESI suggests that S=2 is appropriate. We reached this conclusion by examining the ratio of several key characteristic dimensions in ESI (Table 2) to the expected counter parts in WFOS. Averaging the first four entries returns a value of S=2.0.

	Global Averages	
	microns	arc seconds
-X gravity	140.2	15.9
-Y gravity	219.7	10
-Z gravity	80.9	14.5
Global Avg	147	13

Table 3. Reduced ESI flexure predictions

3.3 ESI Flexure predictions for WFOS analysis

The inputs to the FCS tool are scaled displacements and rotation based on ESIs performance and the choice of scale factor. For $S = 2$ we are scaling ESI deflection by 4 (S^2) and the rotations by 2 (S). The WFOS FCS tool uses local Zemax coordinate systems, rather than a global coordinate system, which are aligned with the axis of each optic. This default mode of Zemax forces the Z axis to be aligned along the central field point chief ray with X and Y axis on the face of each the optic with an arbitrary Z rotation. Because the FCS tool Zemax coordinate system is rotating on each optic, we are randomizing all 6 degrees of freedom by the same magnitude. If we had been using a global coordinate system aligned with the telescope we would have weighted the two axis in which the instrument rotated more heavily. Using ESI as a starting point we start with the X gravity vector case and average the full range of the displacement for each optic for all six degrees of freedom (Ux, Ux, Uz, Rot x, Rot y, and Rot z) . The averages all optics in the direction Ux, Uy and Uz are then averaged again to get a global average displacement for gravity in X. The X, Y and Z gravity deflection and rotation value are then averaged to get a single global average for the deflections and rotations Table (3). If we apply the scale factor of two (S=2) to the ESI results we would expect defections and rotations in WFOS to be approximately 0.6 mm (147 microns x 4) and 26 arc seconds (13 x 2).

4. FLEXURE COMPENSATION SIMULATION TOOL

Flexure Compensation and Simulation (FCS) tool is a flexure modeling tool written in Python to accurately simulate the effects of instrument flexure at the WFOS detector plane (e.g image shifts), using perturbation of key optical elements and also derive corrective motions to compensate the image shifts caused by instrument flexure. The tool provides an intuitive graphical interface to introduce perturbations to optical components and simulate flexure and compensation. It also has a script mode that allows to run monte-carlo simulations of flexure compensation on different optical designs.

4.1 Steps in FCS Modeling

The main steps in the FCS modeling using FCS tool is as follows

1. Derive Sensitivity maps of the components (Collimator, Dichroic etc.) from the Zemax design setting up coordinate breaks.
2. Setup the FCS tool and simulate flexure effect for random combinations of flexure of individual components within the range of motion.
3. Compensation of flexure for a choice of active elements using a merit function and calculate residual image motion.
4. Global optimization routine find the optimal parameter solution for compensation using basin hopping algorithm.

The two main parts of flexure compensation tool are:

4.1.1 Simulation of flexure

Here, we aim to accurately simulate the instrument flexure using ZEMAX sensitivity maps. A sample sensitivity map for different degrees of freedom of the collimator in Xchange-WFOS design is shown in Figure 3 . Simulation of image motions and other effects of flexure are useful for both closed or open loop compensation designs. Hence it is an important step irrespective of the method being adopted for compensation. Simulations of flexure related image motion also helps in the structural design of WFOS. When modeling the effect of instrument flexure at the detector plane we only consider image motion as the only possible effect of flexure. We do not consider defocus, image degradation, vignetting, scattering and other effects. Image shift is still one of the main factor in driving the FCS design, other effects will have only a minor impact on the instrument performance and the science goals. A grid of sensitivities for 260 image positions at the detector are considered in the simulations. The shift due to flexure is modeled as below

$$\begin{aligned} x_i^{flex} &= x_i^{ini} + f_{coll.dx}.\Delta x_i^{coll.dx} + f_{coll.dy}.\Delta x_i^{coll.dy} + ... + f_{mirr.ty}.\Delta x_i^{mirr.ty} + f_{mirr.tz}.\Delta x_i^{mirr.tz} \\ y_i^{flex} &= y_i^{ini} + f_{coll.dx}.\Delta y_i^{coll.dx} + f_{coll.dy}.\Delta y_i^{coll.dy} + ... + f_{mirr.ty}.\Delta y_i^{mirr.ty} + f_{mirr.tz}.\Delta y_i^{mirr.tz} \end{aligned} \tag{3}$$

where x_i^{flex} is the shifted x position due to flexure for the i^{th} sampled point on the spectra, x_i^{ini} is the initial position of the sampled point, $f_{coll.dx}$ is the flexure movement for collimator in the dx degree of freedom and $\Delta x_i^{coll.dx}$ is the image shift in x axis of the detector due to unit shift of collimator in dx. The equation spans over all the components in the optical train of the spectrograph and their 6 degrees of freedom $[dx, dy, dz, tx, ty, tz]$. The other variables in the equation can be similarly inferred.

4.1.2 Compensation and corrective motion

The current flexure compensation scheme uses simulated image motion to derive corrective compensation. Simulated data over the entire detector (260 points) is considered in deriving the compensation motion for a open loop simulation. In the case of a close loop system, image shifts are measured by separate flexure compensation detectors that are (most often) located at the periphery of the science detectors. The FCS tool has provision to choose the simulated data that are located at the periphery of the science detector to represent a close loop compensation scheme. The compensation tool derives corrective motions for various choice of optical components (called as active elements) that will of bring back image to its original nominal position. A global optimizer is used explore the parameter space for compensation. The cost function for the optimization is given below.

$$C_{comp} = \left[\sum_{i=1}^{n_{red}} \sqrt{(x_i^{comp} - x_i^{ini})^2 + (y_i^{comp} - y_i^{ini})^2}\right]^{red} + \left[\sum_{i=1}^{n_{blue}} \sqrt{(x_i^{comp} - x_i^{ini})^2 + (y_i^{comp} - y_i^{ini})^2}\right]^{blue}. \tag{4}$$

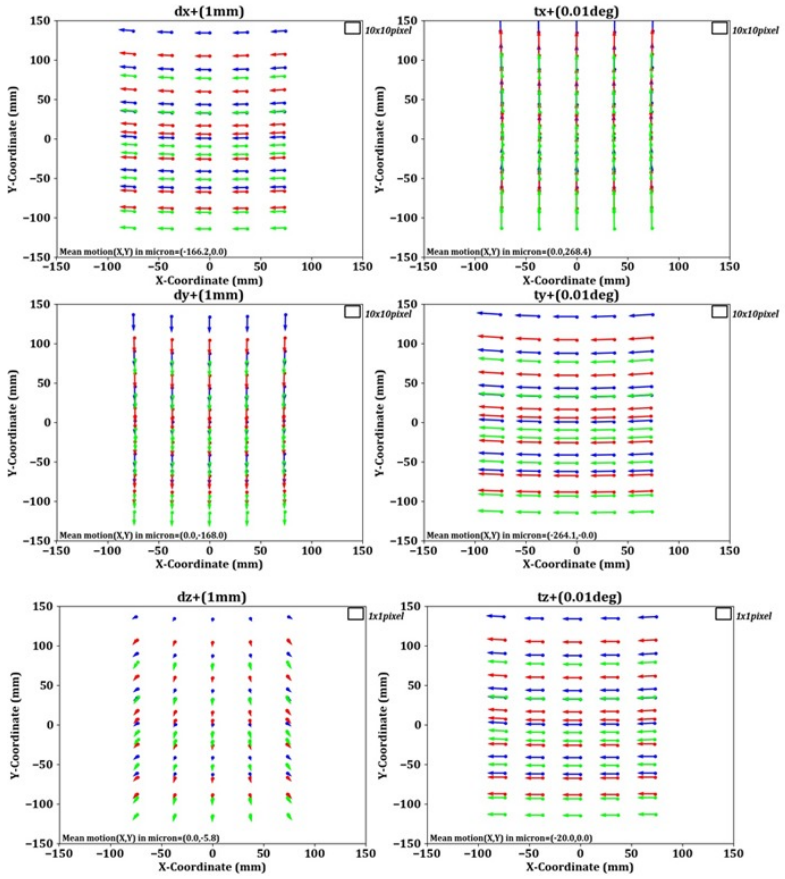

Figure 3. The sensitivity maps of the collimator for unit displacements and tilts across different degrees of freedom [dx,dy,dz,tx,ty,tz]

4.2 Optimization Algorithm

The optimization algorithm used for the tool is the basin hopping algorithm. It is a stochastic optimization algorithm.[7] We use the Scipy optimization library for the basin hopping routines. Earlier version of the tool worked with the simulated annealing routine of Scipy which got deprecated after version 0.14.0 . The basin hopping routine implemented using Scipy is highly customizable to have custom acceptance tests, steps and bounds.

The basinhopping algorithm works at 3 levels. First is a random jump in the variable space. Secondly, a local minimization routine is used to find the local minima. Finally, minima is accepted or rejected based on either metropolis criterion or a custom criteria. Currently Scipy based L-BFGS is used as a local minimizer.

4.3 Features

The interface for the tool is shown in Figure 4 and Figure 5. The GUI and the back-end algorithms are all implemented using Python. The current version of the tool, uses a grid of models generated using ZEMAX for a known amount of flexure of key optical components (called the sensitivity maps). These pre-calculated grid of sensitivity maps are used to generate various combinations perturbations and a realistic image motion due to flexure. This approach has certain advantages:

1. Reduced computing time.

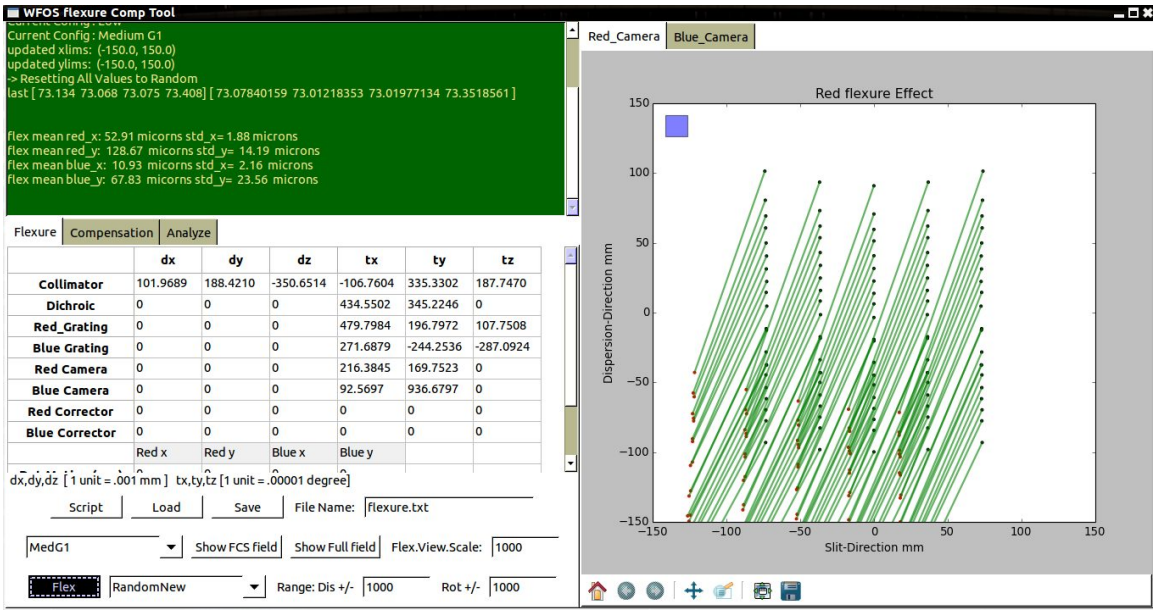

Figure 4. The flexure compensation tool interface

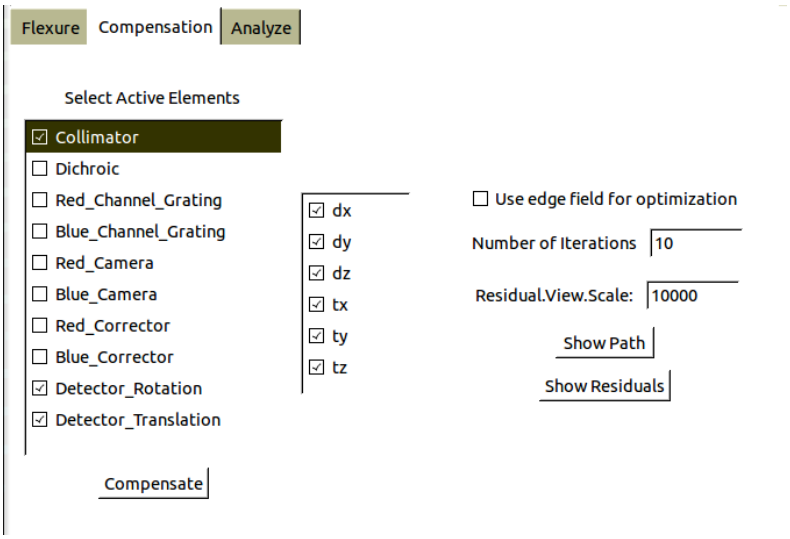

Figure 5. The compensation tab of the tool

2. Standalone tool that does not require further ray tracing. So, ZEMAX or any other ray tracing code is not needed, once we have the pre-calculated sensitivities. The tool is developed using python and is an open-source software.

3. To derive compensation and correction, sensitivities for several realizations of optical configuration are needed . In this approach, same pre-calculated ZEMAX grid of models will be used for compensation of flexure as well.

Some of the limitations of this method could arise from the accuracy of the models, due to the field dependency and nonlinearity of the sensitivity maps. This will be of the order of the derivative of optical distortion between two positions of the grid points at the detector. This can be certainly improved by increasing the grid points. We discuss the preliminary results of the validation of the tool, assumptions and limitations and finally lists the

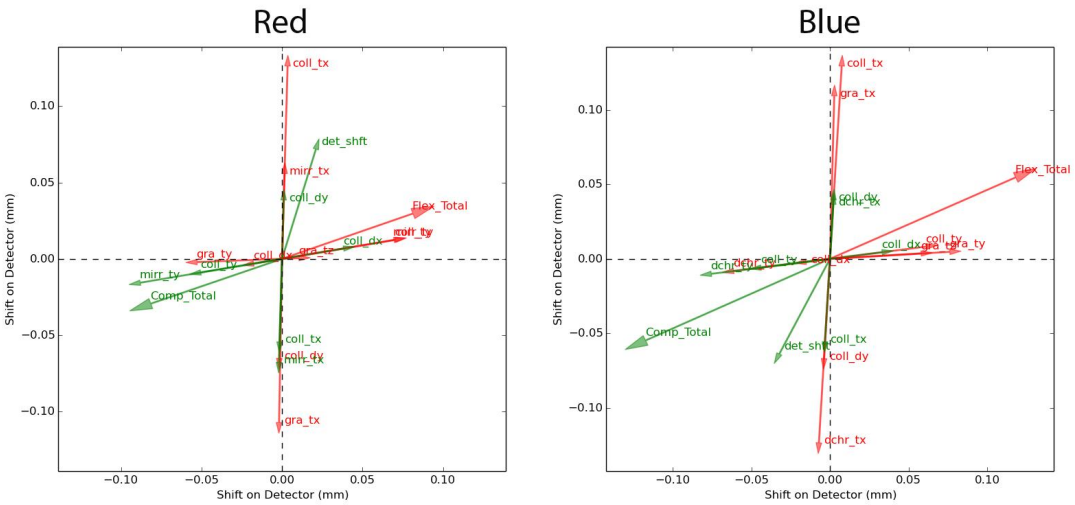

Figure 6. The flexure and compensation vectors for the main optical components for one set of the flexure realization.

possible sources of error. Similar modeling approach that does not use a pre-calculated grid, may need ZEMAX or some ray-tracing tool along with an optimization routine to derive compensation motion at each instant. This will require large computation time. One of the main drawback of a non-grid based approach is the need for large number of fresh ZEMAX runs to derive accurate global minima each time. This is not an issue for a pre-calculated grid approach.

In the current work, a grid of sensitivities was calculated for key optical elements of WFOS (collimator, dichroic, corrector lenses and gratings). Key optical elements were perturbed in 6 degrees of freedom (displacement and tilt about XYZ axis) and its sensitivity to image motion on the detector plane were recorded. Vector plots of the image motions for each of the elements are also viewable with the tool as shown in Figure 6. Sensitivity maps cover the full WFOS detector, by including several input field positions and list of fiducial wavelengths. Sensitivity maps were calculated for 0.01 degrees tilt and 1mm displacement of the optical elements, these maps were called 1x sensitivity maps. The values of flexure (1mm & 0.01 degrees) used here are based on the scaling of similar instruments on the 8-10m telescopes to WFOS, primarily ESI on Keck.

Based on sensitivity maps of individual optical elements, we identify some of the degenerate states of the system. Due to the degenerate motions of optical elements, it may be possible to compensate the image motion caused by flexure of the entire instrument, using fewer corrective (active) elements. We minimize the distance of the image motions between the original/nominal positions to the shifted/flexed position at the detector to derive the corrections (called as penalty function). Since there is two color channels in WFOS, there are common and separate light paths for different optical elements, this requires simultaneously optimizing the image shifts in both channels to derive corrections. We also developed a flexible graphic interface for users to use this modeling too

4.4 Modeling and Assumptions

Simulation of flexure is modeled by simple vector addition of image shifts caused by perturbation of individual optical elements. Sensitivities of optical components are calculated by the image shifts caused by perturbing the optical elements with respect to unperturbed nominal position by an amount 1mm/0.01 degrees. Some of the assumptions of this modeling are:

1. All perturbations to optical elements are applied at the same instant. The order in which the perturbation happens is assumed to have no effect. This assumes commutativity of operations and no dependency of initial starting point. In reality, the flexure can be random combinations of perturbation in any order. However, due to the ray-trace path automatically a sequence is assumed between the optical elements.

This can be noticed from the sensitivity maps, the final pattern of the image motion is mainly due to the grating. Perturbations of other optical elements before the grating change the input angles at the grating and that decides the resultant pattern. For a case of a given optical element, ZEMAX considers a sequence between translation and rotation motions. ZEMAX by default considers rotation first before translation, unless it is specified. The effect of sequence of rotation and translation has no significant effect for 1x (1mm translation, 0.01deg tilt) to 10x perturbation range.

2. Another error that can come is the field dependency of sensitivity. Flexure is calculated as a vector addition of all individual perturbations, but these individual perturbations are calculated with respect to the nominal unperturbed positions. However, in a real situation, a sequence of perturbations will have different starting nominal positions. This can be imagined as having a starting point at different field position? Because of the field dependency of distortion sensitivities, there may be an error. These are not considered now. This can be implemented easily in the next phase. This will have only a minor effect,which will be of the order of derivative of distortions between two grid points that are considered in the input sensitivities. For the 1x range it is found to be 1-3microns.

3. Linearity of sensitivities are assumed, in the range 0-1mm and 0-0.01deg. This is a reasonable assumption. Linearity of the sensitivities, between 1x(1mm displacement and 0.01 degree tilt) and 3x (3mm displacement and 0.03 degree tilt) range is shown in Figure 7, by calculating difference between the sensitivity data for 3x and 3 times 1x sensitivities. The purple box shows the size of 1 pixel (15x15microns). The rms residual is 3.4290 microns and maximum residual is 10 microns. The linearity and field dependency have the same same source of error. These values are approximately three times the difference between ZEMAX and FCStool for 1x perturbations. So, we think either including more number of field locations or calculation of sensitivity grids for several scaling and using interpolation will reduce these errors.

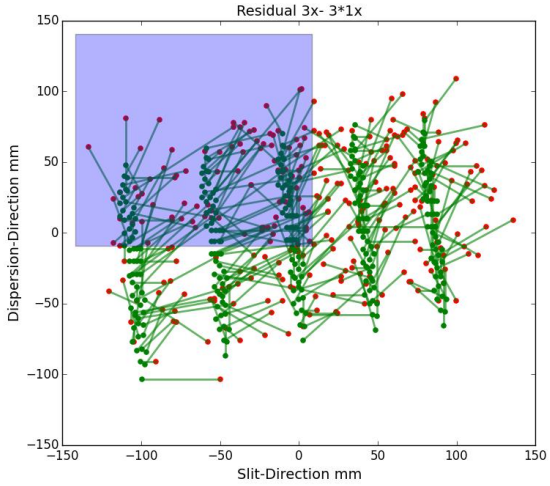

Figure 7. Difference residual between flexure induced image motion with 3x sensitivity motion and 3 times 1x sensitivity motion.

5. VALIDATION

We present preliminary results of validation of the FCS simulation. These tests was done on the OMDR-WFOS design. For three sets of random perturbation of all the key elements, the sensitivity maps are compared with that of ZEMAX results. These tests cover three different range of perturbations (scale-0.1x, scale-0.5x, scale-1x), listed in the tables. Scale-0.1x corresponds to 0-0.1x range for perturbation (0-0.1 mm displacements and 0-0.001 degree tilts) , scale-0.5x is 0.5x (0-0.5 mm displacement and 0-0.005 degree tilt) and scale-1x is 1x (0-1mm

Element	dx	dy	dz	tx	ty	tz
Collimator	31.8505	86.6833	97.762	67.5209	-40.506	73.5696
Mirror	-25.2141	-39.3645	39.8278	-84.4402	86.948	85.5888
Dichroic	53.716	23.4046	36.9393	-39.1687	-94.2845	-27.9702
Red_Grating	-12.6528	41.6951	97.973	49.0754	17.7727	-65.7572
Blue_Grating	52.665	2.188	-84.9307	-54.1342	43.0741	-3.7837

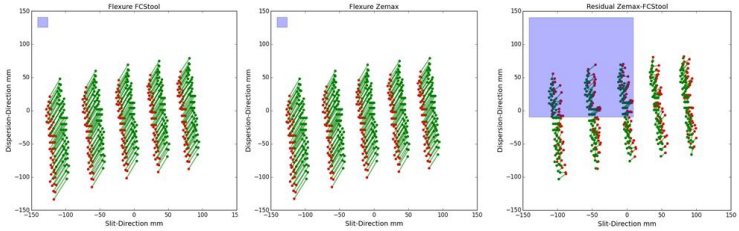

Figure 8. Zemax Validation Results with Scale 0.1x. The top panel shows the values of flexure of each component in flexure units. [1000 units= 1mm/0.01 degree]

Element	dx	dy	dz	tx	ty	tz
Collimator	-159.257	391.456	16.2666	80.4936	106.2936	-312.3719
Mirror	418.3236	-359.419	-159.0738	-151.0266	48.2331	-134.7116
Dichroic	138.9794	414.1425	419.7775	-199.3857	-273.7813	-409.6948
Red_Grating	-239.1331	471.9542	-266.8725	-200.8221	-13.9383	-47.9617
Blue_Grating	212.3695	115.0311	-457.222	97.3991	233.6718	-135.0832

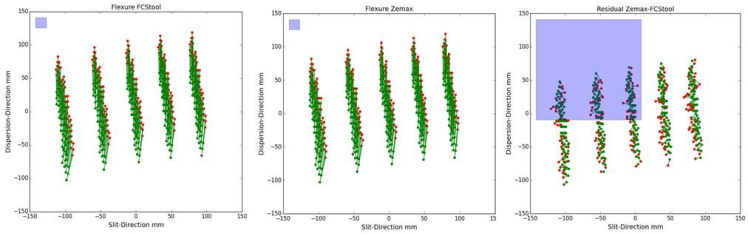

Figure 9. Zemax Validation Results with Scale 0.5x.

displacement and 0-0.01 degree tilt). Figure 8, Figure 9 and Figure 10 show a comparison of sensitivity patterns and the difference between image shifts calculated by ZEMAX and FCStool. FCStool assumes linear vector sum of perturbation of individual elements from same initial locations. Some of the assumptions are discussed in the previous section, due to which one would expect difference between ZEMAX and FCStool.

Overall, the sensitivity patterns from FCStool and ZEMAX matches well for all the random perturbations of different ranges. We find the residuals are about 1-4microns, in the range of 1x perturbation, See Table 4. The residual error between ZEMAX and FCStool does not change between scale 0.1x scale 0.5x simulations, this may be due to linearity and non field dependency in this range of perturbation. However, it clearly increases for the scale 1x. This could be due to the field dependency and assumption of same nominal location, which can be improved in the future. The numerical accuracy of the input sensitivities itself is only 1 micron. In the future updates we will include better numerical precision of the grids of sensitivities generated using ZEMAX. For now we are satisfied with the model accuracy and residual errors because the scaling estimate from ESI suggests that the expected displacements of Xchanger WFOS will be 0.6mm.

Flexure Scale	Bulk Motion (μm)	Residual RMS (μm)	Maximum Residual (μm)
Scale 0.1x	27.61	0.718	1.444
Scale 0.5x	37.85	0.612	1.353
Scale 1x	345.9	1.677	3.696

Table 4. The rms residuals and maximum residuals after subtraction of Zemax and FCS Tool image motion for different ranges of perturbations

Element	dx	dy	dz	tx	ty	tz
Collimator	-534.3432	-674.3743	-112.4586	597.981	-447.0803	357.2287
Mirror	546.9691	254.949	-10.52	222.0085	-724.3244	-779.7016
Dichroic	409.2881	-975.3178	839.4284	754.3414	-754.6764	614.0178
Red_Grating	618.7307	-46.076	170.8187	773.1869	153.1686	619.6498
Blue_Grating	555.735	-116.04	461.0169	-137.3937	666.4868	368.1794

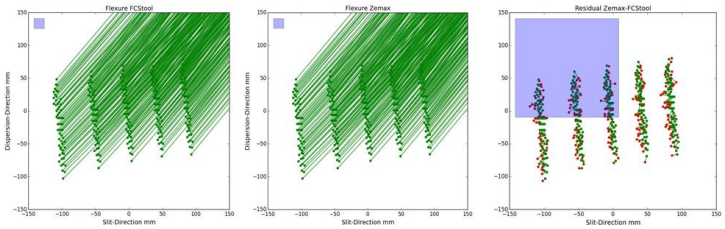

Figure 10. Zemax Validation Results with Scale 1x.

6. ANALYSIS

The flexure compensation tool was used to analyze TMT-WFOS designs that were developed during the conceptual design phases. The tool has an automated scripting mode that allows us to run random realizations of different flexure values of a range. This mode is used to run monte-carlo simulations of flexure compensation. The analysis for the Xchange-WFOS design is shown in Figure 11. As can be observed from the simulations, the compensation with detector alone restricts the mean residuals to within the 1 pixel requirement which is the requirement to for Xchanger WFOS to be GLAO(Ground Layer Adaptive Optics) ready. Although the maximum residuals in each run are over the 1 pixel GLAO limit the results are much better for the 2 pixel seeing limited requirement which is the operational requirement for the foreseeable future.

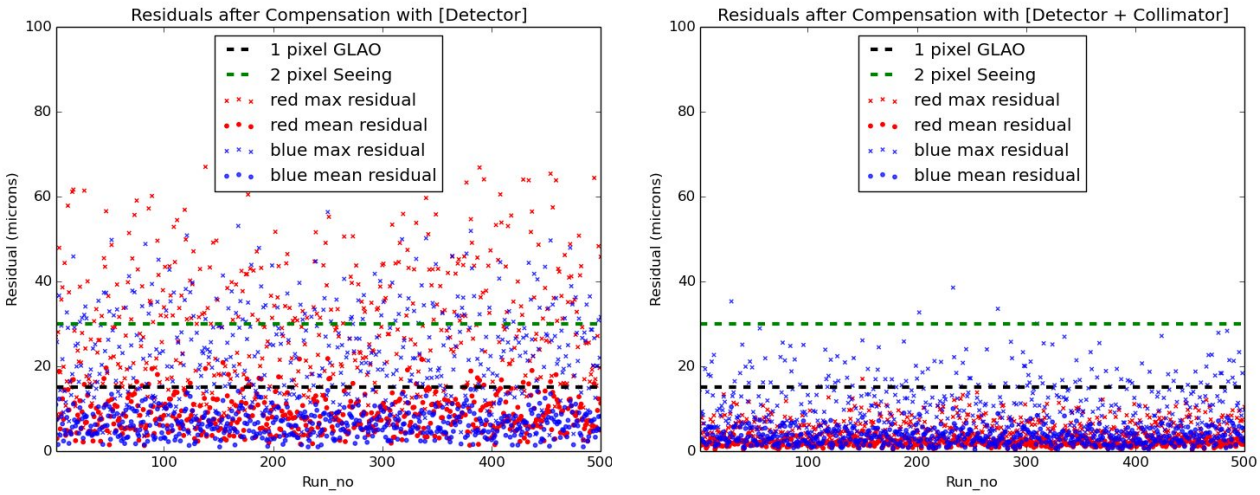

Figure 11. Residuals after monte carlo simulations of flexure compensation. [Left] Compensation using only detector as an active element. [Right] Compensation using collimator and detector as active elements for the compensation scheme.

7. CONCLUSIONS

We discussed the implementation of a flexure compensation tool used to analyze and design different schemes of compensation for flexure related image motion in TMT-WFOS Instrument. The tool provides a graphical interface to simulate the effect of flexure in major optical elements of the instrument and also to derive compensation using few active elements. The tool has been used to analyze the flexure compensation of Xchanger

design of TMT-WFOS and to provide useful insights for the design of a flexure compensation system for such an instrument. The tool can be easily adapted to other spectrographs for similar studies.

ACKNOWLEDGMENTS

The TMT Project gratefully acknowledges the support of the TMT collaborating institutions. They are the California Institute of Technology, the University of California, the National Astronomical Observatory of Japan, the National Astronomical Observatories of China and their consortium partners, the Department of Science and Technology of India and their supported institutes, and the National Research Council of Canada. This work was supported as well by the Gordon and Betty Moore Foundation, the Canada Foundation for Innovation, the Ontario Ministry of Research and Innovation, the Natural Sciences and Engineering Research Council of Canada, the British Columbia Knowledge Development Fund, the Association of Canadian Universities for Research in Astronomy (ACURA), the Association of Universities for Research in Astronomy (AURA), the U.S. National Science Foundation, the National Institutes of Natural Sciences of Japan, and the Department of Atomic Energy of India.

REFERENCES

[1] Walker, D. and D'Arrigo, P., "On the stability of Cassegrain spectrographs," *mnras* **281**, 673–678 (July 1996).

[2] Kibrick, R. I., Allen, S. L., Clarke, D. A., Faber, S. M., Phillips, A. C., and Wirth, G. D., "The DEIMOS flexure compensation system: overview and operational results," in [*Ground-based Instrumentation for Astronomy*], Moorwood, A. F. M. and Iye, M., eds., *procspie* **5492**, 799–810 (Sept. 2004).

[3] Sheinis, A. I., Bolte, M., Epps, H. W., Kibrick, R. I., Miller, J. S., Radovan, M. V., Bigelow, B. C., and Sutin, B. M., "ESI, a New Keck Observatory Echellette Spectrograph and Imager," *pasp* **114**, 851–865 (Aug. 2002).

[4] Bigelow, B. C., Radovan, M. V., Bernstein, R. A., Onaka, P. M., Yamada, H., Isani, S., Miyazaki, S., and Ozaki, S., "Conceptual design of the MOBIE imaging spectrograph for TMT," in [*Ground-based and Airborne Instrumentation for Astronomy V*], *procspie* **9147**, 914728 (Aug. 2014).

[5] Rebecca A. Bernstein, B. C. B., "An optical design for a wide-field optical spectrograph for tmt," (2008).

[6] Bundy, K. et al., "WFOS instrument trade study: slicer vs. fiber instrument concept designs and results," in [*Proc. SPIE, 10702, in press (2018)*], *procspie* **10702** (2018).

[7] Wales, D. J. and Doye, J. P. K., "Global optimization by basin-hopping and the lowest energy structures of lennard-jones clusters containing up to 110 atoms," *The Journal of Physical Chemistry A* **101**(28), 5111–5116 (1997).